Reaction of a Cr Atom with H_2, N_2, and O_2: A Density Functional Study

Ana Martínez

Departamento de Química, División de Ciencias Básicas e Ingeniería, Universidad Autónoma Metropolitana-Iztapalapa, A.P. 55-534, México D.F. 09340, México

Received: August 22, 1997; In Final Form: November 20, 1997

The study of the reaction of a Cr atom with H_2, N_2, and O_2 is performed in order to obtain an explanation of the different observed reactivities. The reactivity is investigated with the all-electron linear-combination-of-Gaussian-type-orbitals Kohn−Sham density functional theory (LCGTO-KS-DFT). The equilibrium geometries are characterized by their binding energies and harmonic frequencies. For CrH_2, the lowest minimum is a quintet bent structure. The binding energy with respect to Cr + H_2 is 6.7 kcal/mol, and the electronic state is $^5B_1$. For CrN_2, the lowest minimum is a septet linear structure. The binding energy with respect to Cr + N_2 is 4.8 kcal/mol, and the electronic state is $^7\Sigma^+$. For CrO_2 several local minima on different potential energy surfaces were obtained. The lowest minimum for CrO_2 is a bent structure on the triplet potential energy surface. The binding energy with respect to Cr + O_2 is 125.6 kcal/mol, and the electronic state is $^3B_2$. A detailed analysis of the molecular orbitals for the most stable structures is given. As the mechanism of the reaction, a two-step charge-transfer process is suggested, were the Cr atom is always the electron donor. The theoretical explanation of some of the available experimental results provides a better understanding of the electronic structure and the reaction mechanism.

Introduction

The reactivity of small transition-metal clusters is a topic of major interest because transition metals have a rich and varied chemistry and play an important role in numerous chemical systems. These clusters can be used as models in the study of the reactivity of metal centers in catalytic processes. The study of the bonding on metal−ligand systems has applications in many fields.[1,2] For example, the investigation of N_2 chemisorption on transition-metal clusters provides a possibility to improve our understanding of the factors that influence the important nitrogen fixation process. The investigation of physisorption and chemisorption on clusters, as well as the incorporation of atoms and molecules into clusters,[3−7] has become possible due to the spectacular progress in cluster research. The developments on theory and experiments are providing valuable information on many properties of atomic aggregates.

Despite the importance of transition metals, relatively little is known about the detailed reactivity of transition-metal atoms with small molecules. There are many theoretical works about the reaction of transition-metal atoms with the hydrogen molecule.[8−20] The theoretical information about these systems can be summarized as follows: (i) it is necessary to include electron correlation when the problem of the dissociation of H_2 is studied; (ii) the metal atom is more able to react if it is present in the $d^{n-1}s^1$ configuration than in the $d^{n-2}s^2$ configuration; (iii) there are two possible bonding situations, bent (C_{2v} symmetry) and linear ($C_{\infty v}$ symmetry) structures; for the bent complexes, the formation of "sd" hybrid bonds is important; in both complexes, the d orbitals play an important role in the dissociation reaction; (iv) relativistic effects may influence the strength of the M−H bond (for example, when the comparison between Pd and Pt is made); and (v) the reaction is different when the metal atom is ionized. Some of these factors could also be important for reactions of the Cr atom.

For the reaction of N_2 with transition metals, the experimental information of particular relevance for this work can be summarized in two points: (i) the dissociation of N_2 with small or no energy barriers is only possible with metals that have open d orbitals, and (ii) Fe and Cr are able to dissociate N_2, whereas Ni and Co do not present dissociative reactions. The difference between different metals in their ability to react with N_2 must be explained with a systematic study of the electronic structures of the metal and the molecule. Following this idea, Siegbahn and Blomberg[21] performed a theoretical study using the complete active space self-consistent-field method, followed by multireference contracted CI calculations. They reported that the more stable structures are in the end-on approach, in agreement with most of the metal complexes that are well-characterized experimentally. More recently, Bauschlicher et al.[22] reported a CASSCF study of FeN_2, FeCO, and Fe_2N_2, finding similar reactivity behavior of N_2 and CO in the side-on bonding geometry.

Recently, Parnis and co-workers[23] reported an experimental study about the reaction of transition-metal atoms with small molecules. They used the technique of gas-phase metal atom formation by visible multiphoton dissociation of a volatile organometallic compound. Using this technique, they studied main group metal atom reactions with a variety of simple molecules.[23−27] In particular, they examined the reactivity of ground-state ($^7S_3$) Cr atoms with small molecules. They found that the dominant feature of Cr atom chemistry is the formation of association complexes with the stable free radicals O_2 and NO. For the reaction between the Cr atom and closed-shell molecules low reactivity was found. The interpretation of this behavior was given in terms of repulsive interactions involving the valence s electron on Cr.

In a previous work[28] we investigated the reactivity of a Mo atom with H_2, N_2, and O_2. We used MoH_2 to validate the DFT methodology, comparing with accurate relativistic CI results.[16]

S1089-5639(97)02747-3 CCC: $15.00
Published on Web 01/30/1998

The reactions of a Mo atom with N_2 and O_2 were studied in order to obtain an explanation of the different experimental reactivities reported by Lian et al.[29] We found that the different reactivities of N_2 and O_2 with the Mo atom are due to the different bond strengths of these molecules. For the MoO_2 system, the O_2 molecule is completely dissociated after two spin flips, and the Mo−O bonds are formed. For the MoN_2 system, the thermodynamically unstable side-on complex was found to be the product of the reaction, even after two spin flips. The Mo atom is always the electron donor in these reactions.

To explain the behavior of the Cr atoms with some small molecules, a density functional study of the interaction of the Cr atom with H_2, N_2, and O_2 was performed. Bond distances, equilibrium geometries, binding energies, harmonic frequencies, and electronic states for CrH_2, CrN_2, and CrO_2 are reported in order to study the reactivity of the Cr atom. For these systems, as a consequence of a charge-transfer process, the spin flips and the bond is formed. The Cr atom is always the electron donor. For CrH_2, the ground state is a quintet bent structure. For CrN_2, the ground state is a septet linear structure. After one spin flip, the thermodynamically unstable side-on complex as the product of the reaction was found. For CrO_2, the O_2 molecule is completely dissociated after two spin flips, and the Cr−O bonds are formed. With these results, a comparison and explanation of the available experimental results are given. A detailed study of the molecular orbitals and a comparison with the reactivity of the Mo atom are also given.

Computational Details

The program package deMon-KS[30] and deMon-properties[31] were used to perform all the calculations. The linear-combination-of-Gaussian-type-orbitals Kohn−Sham density functional theory (LCGTO-KS-DFT) is implemented in this program. The local spin-density approximation (LSD) of density functional theory (DFT) was included as in Vosko, Wilk, and Nusair,[32] while generalized gradient approximation (GGA) calculations used the gradient terms of Perdew and Wang for exchange[33] and Perdew for correlation.[34,35] Full geometry optimization was performed at the LSD level, and the GGA potential was included self-consistently for the final energy evaluation. The common practice of running GGA single-point energy calculations at a geometry computed at the LSD level was used before.[28] As it was reported, optimized geometries at the LSD level are in good agreement with experimental values and with other theoretical results. For the final energy evaluation it is important to include the GGA corrections.

The Gaussian orbital basis sets[36] that we have used are (63321/5211*/41+) for chromium, (41) for hydrogen, (621/41/1*) for nitrogen, and (621/41/1*) for oxygen. The auxiliary funtion set used to fit the charge density and the exchange−correlation potential is (5,5;5,5) for chromium, (4;4) for hydrogen, (4,3;4,3) for nitrogen, and (4,3;4,3) for oxygen. In this notation, the charge density and the exchange−correlation auxiliary function sets are separated by a semicolon. Following the notation (k_1,k_2;l_1,l_2), the number of s-type Gaussians for the charge density (exchange−correlation) fit is represented by k_1 (l_1), while k_2 (l_2) gives the number of s-, p-, and d-type Gaussians in the charge density (exchange−correlation) auxiliary function set. To study the influence of polarization functions on the hydrogen atoms, we also used a (41/1*) basis set in combination with a (4,2;4,2) auxiliary function set for the H atom. Our calculations showed that the contribution of the polarization functions in the MOs of the CrH_2 and the Mulliken population of these functions are negligible.

TABLE 1: Some Electronic Configurations of the Cr Atom and Their Energies Relative to the Ground State[a]

atomic configuration of Cr	ΔE (kcal/mol)		
	expt[b]	LSDA	GGA
$3d^54s^1(^7S)$	0.0	0.0	0.0
$3d^54s^1(^5S)$	21.71	26.32	23.24

[a] Results at the LSD level (Vosko, Wilk, and Nusair[32]) and at the GGA level (Perdew and Wang for exchange[33] and Perdew for correlation[34,35]) and some experimental data.[40] [b] Experimental data from ref 40.

The charge density was fitted analytically, while the exchange−correlation potential was fitted numerically on a grid[37] (deMon option FINE)[30] composed of 32 radial shells and 26 angular points per shell.[37] At the end of each SCF procedure, the exchange−correlation contribution to the energy gradients was calculated by numerical integration on an augmented set of grid points consisting of the same 32 radial shells with 50, 110, or 194 angular grid points.

Full geometry optimizations without symmetry constraints have been performed, starting from several initial geometries to locate different minima on the potential energy surface (PES). Geometries were optimized using the method of Broyden−Fletcher−Goldfarb−Shanno (BFGS)[38] or the conjugate gradient method.

To discriminate minima from other critical points on the potential energy surface, a vibrational analysis was performed using numerical differentiation (two-point finite differences) of the gradients, using a displacement (GSTEP) equal to 0.02 au and a density convergence threshold equal to 10^{-6}. The effects of the GSTEP and the density convergence threshold in vibrational analyses have been discussed elsewhere.[39] Since the geometries were optimized at the LSD level, the vibrations were calculated in the LSD approximation too. The total energies (available on request) include the GGA corrections.

Results and Discussion

In Table 1, some selected electronic configurations of the Cr atom and their relative energy differences from the ground state are presented. The results at LSD and GGA levels are compared with experimental data.[40] The electronic ground-state configuration (d^5s^1) that was found is the same as the experimental one. The calculated energy differences relative to the ^7S ground state are bigger than the experimental ones by 2−5 kcal/mol. This error is small enough for a reliable assignment of the atomic states of the Cr atom.

A. Geometry Optimization of CrH_2. In Figure 1, the optimized geometries for CrH_2 are presented. As discussed above, these geometries are fully optimized at the LSD level. Bond distances at the LSD level and energy differences at the GGA level with respect to $Cr(^7S) + H_2$ are also shown. For CrH_2 the most stable spin multiplicity is the quintet, which lies 6.7 kcal/mol under the dissociation limit of the separated Cr(^7S) atom and H_2 molecule. The formation of two Cr−H bonds has reduced the multiplicity; the magnetic moment of the system is reduced by 2 μB (see ref 41 for other examples of the interplay between chemisorption and magnetism). The ground state is a bent structure, where the H_2 molecule is completely dissociated. On the quintet PES, a linear structure that is 16.0 kcal/mol less stable than the dissociation limit was also found. In Figure 1 a bent structure on the triplet PES can be seen. However this state is less stable than the quintet and lies 24.0 kcal/mol above the dissociation limit. The lowest singlet state is a bent structure. When this geometry was optimized, fractional occupation

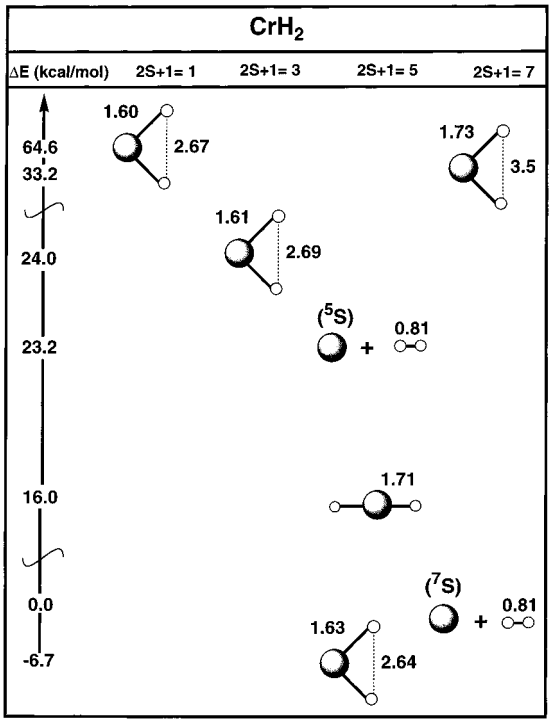

Figure 1. Optimized geometries of CrH_2 for different spin multiplicities. The geometries were obtained at the LSD level (Vosko, Wilk, and Nusair[32]), by minimization of the total energy, without symmetry constraints. Bond distances (in Å) and energy differences (in kcal/mol) at the GGA level (Perdew and Wang for exchange[33] and Perdew for correlation[34,35]) are also shown. The GGA results are single-point calculations with the geometry optimized at the LSD level.

numbers were used in order to obtain convergence. For this system, the calculation with integer occupation numbers was not tested because it is a highly excited state that lies 64.6 kcal/mol above the dissociation limit.

Figure 1 shows two dissociation limits, one on the quintet and the other on the septet surface. The energy difference between these two systems is due to the different electronic configurations of the Cr atom.

A vibrational analysis was performed in order to ensure that the optimized geometries are minima on the potential energy surface. In Table 2, molecular structures, spin multiplicities, relative energies at the LSD and GGA levels, harmonic frequencies, and the assignment by symmetry of the most stable geometries of the triplet and quintet states are summarized. As it can be seen, the stability order is the same at the LSD and GGA levels. The vibrational analysis was obtained at the LSD level. The calculated frequencies indicate that the quintet and triplet bent structures are minima. The vibrational analysis of the quintet linear structure was also performed. The calculated frequencies (not in Table 2) indicate that this structure could be a transition state. There are two negative normal modes. The two imaginary frequencies are degenerate, and the movements correspond to the displacement of the hydrogen atoms out of the line (one in the *xz* plane and the other in the *xy* plane) If this system is a transition state, the movements of the atoms will lead to two symmetry-equivalent structures, perpendicular to each other. In this sense, this structure could be a transition state.

The calculated frequencies in Table 2 indicate that all the structures have similar metal−hydrogen bonding. To a first approximation the differences in the electronic structure of these systems involve changes in the spin state of the Cr atom only.

TABLE 2: Molecular Structures, Spin Multiplicities, and Relative Energies (in kcal/mol) at the LSD Level (Vosko, Wilk, and Nusair[32]) and at the GGA Level (Perdew and Wang for Exchange[33] and Perdew for Correlation[34,35]), Harmonic Frequencies (in cm^{-1}), and the Assignment by Symmetry of the Most Stable Geometries of Quintet, Septet, and Triplet Spin States of CrH_2[a]

Structure	2S+1	ΔE(LSD) (Kcal/mol)	ΔE(GGA) (Kcal/mol)	ν (cm^{-1})	A
1.63 2.64	5	-6.2	-6.7	562 1730 1731	a_1 b_1 a_1
0.81 +	7	0.0	0.0		
1.61 2.69	3	28.2	24.0	603 1815 1816	a_1 a_1 b_1

[a] The GGA results are single-point calculations with the geometry optimized at the LSD level. Vibrational studies were performed at the LSD level (Vosko, Wilk, and Nusair[32]).

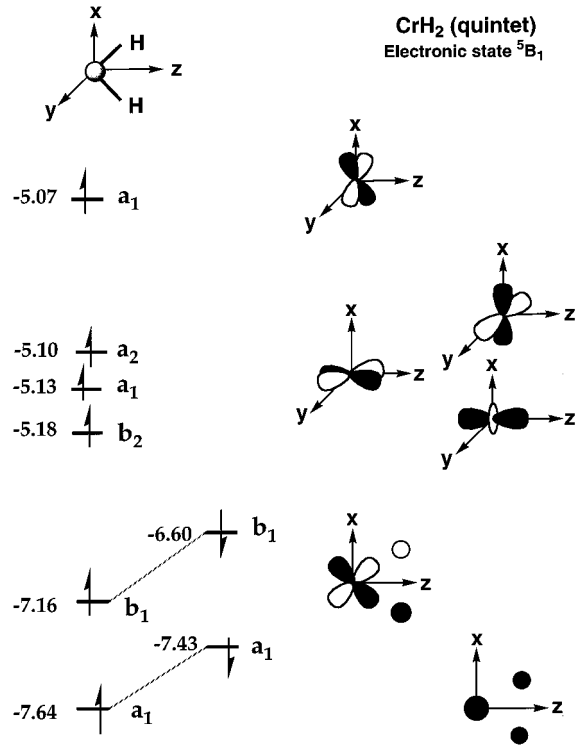

Figure 2. Valence molecular orbital diagram for the ground state of CrH_2. Symmetries, eigenvalues (in eV), and occupation numbers are presented.

Essentially, nonbonding orbitals are involved, which results in similar sets of harmonic frequencies.

In Figure 2 the molecular orbital diagram of the ground state of CrH_2 is presented. The electronic state for this system is $^5B_1$, the singly occupied orbitals being on the Cr atom. The same behavior for MoH_2 was found.[28]

The experimental results of Parnis and co-workers[23] indicate that the reactivity of ground-state Cr atoms with H_2 is not significant, in agreement with the results in Figure 1, where the quintet bent structure appears to be very weakly bonded. Given that the energy difference is quite small, caution is required regarding a definitive theoretical conclusion on the reactivity of Cr with H_2.

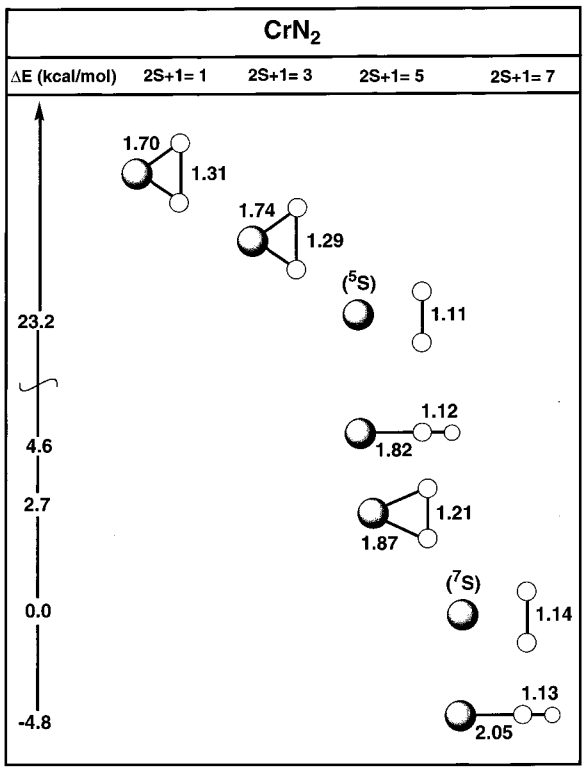

Figure 3. Optimized geometries of CrN_2 for different spin multiplicities. The geometries were obtained at the LSD level (Vosko, Wilk, and Nusair[32]), by minimization of the total energy, without symmetry constraints. Bond distances (in Å) and energy differences (in kcal/mol) at the GGA level (Perdew and Wang for exchange[33] and Perdew for correlation[34,35]) are also shown. The GGA results are single-point calculations with the geometry optimized at the LSD level.

It is interesting to compare the present results for Cr with those for Mo.[28] The behavior of the Cr atom with the H_2 molecule is quite similar to that shown by the Mo atom interacting with H_2. The triplet MoH_2 bent minimum and the triplet CrH_2 bent minimum are both less stable than their dissociation limits. The ground state for CrH_2 and MoH_2 is a quintet bent structure. However, the energy difference between these minima and their dissociation limit is small (10.6 and 6.7 for MoH_2 and CrH_2, respectively), and hence, a definite conclusion is again difficult to reach. For these systems, it could be interesting to perform calculations with highly accurate methods such as CCSD(T).

The reactions and photochemistry of Cr and Mo with molecular hydrogen have been investigated by Xiao et al.[42] The experimental bond angles were estimated to be $118 \pm 5°$ and $110 \pm 5°$ for CrH_2 and MoH_2, respectively, from the relative intensities of the antisymmetric and symmetric streching modes. The theoretical bond angles that we obtained are 108.5° and 104.8° for CrH_2 and MoH_2, respectively, in good agreement with experiment. Both CrH_2 and MoH_2 have been shown to be highly bent molecules, with MoH_2 being slightly more bent than CrH_2. This suggests that Cr and Mo both tend to use d electrons for bonding rather than promoting electrons to p orbitals. The idea of d electrons for bonding rather than promoting electrons to p orbitals is confirmed with the molecular orbital pictures reported before[28] for MoH_2 and in Figure 2 for CrH_2.

B. Geometry Optimization of CrN_2. For this system, several initial geometries and multiplicities were used, and several critical points on the different PES were found. The optimized geometries of CrN_2 are shown in Figure 3. Bond distances at the LSD level and energy differences at the GGA level with respect to the dissociation limit ($Cr(^7S) + N_2$) are also shown.

TABLE 3: Molecular Structures, Spin Multiplicities, and Relative Energies (in kcal/mol) at the LSD Level (Vosko, Wilk, and Nusair[32]) and at the GGA Level (Perdew and Wang for Exchange[33] and Perdew for Correlation[34,35]), Harmonic Frequencies (in cm^{-1}), and the Assignment by Symmetry of the Most Stable Geometries of Septet and Quintet Spin States of CrH_2[a]

Structure	2S+1	ΔE(LSD) (Kcal/mol)	ΔE(GGA) (Kcal/mol)	ν (cm^{-1})	A
1.13, 2.05	7	-5.8	-4.8	185 336 2079	π σ+ σ+
1.14	7	0.0	0.0		
1.21, 1.87	5	-5.6	2.7	501 553 1729	b_1 a_1 a_1

[a] The GGA results are single-point calculations with the geometry optimized at the LSD level. Vibrational studies were performed at the LSD level (Vosko, Wilk, and Nusair[32]).

For the septet states, one minimum was found. It is a linear structure that lies 4.8 kcal/mol under the dissociation limit. The Cr−N bond distance is 2.05 Å, and the N_2 is molecularly bonded to the Cr atom. For the quintet states, Figure 3 shows two different minima with similar stability, the linear and the bent structures, both with the N_2 molecularly bonded to the Cr atom. These structures are less stable than the dissociation limit by 2.7 and 4.6 kcal/mol, for the bent and the linear structures, respectively. The dissociation limit on the quintet PES ($Cr(^5S) + N_2$) is 23.2 kcal/mol less stable than the dissociation limit on the septet PES ($Cr(^7S) + N_2$). This energy difference is due to the different electronic configuration of the Cr atom. On the quintet PES, a bent minimum with the N_2 molecule molecularly bonded was found. This structure is thermodynamically unstable with respect to the septet dissociation limit (2.7 kcal/mol) but stable with respect to the quintet dissociation limit (−20.5 kcal/mol). Hence, if the Cr atom is in an excited quintet state, the reaction between Cr and N_2 leading to a metastable quintet could be possible.

In Table 3, molecular structures, spin multiplicities, relative energies at LSD and GGA levels, harmonic frequencies, and the assignment by symmetry of the most stable geometries of the septet and quintet states of CrN_2 are summarized. For CrN_2 the stability order is not the same at the LSD and GGA levels. It seems that the GGA corrections are more important in this system than in CrH_2. The bonding is different from the CrH_2 system, since the ground state presents the same spin multiplicity as the dissociated ($Cr(^7S) + N_2$) system.

All the energy values reported in Table 3 fall into the "weak interaction" category, similar to the energies of the hydrogen bond or Mulliken charge-transfer complexes[43] and, contrary to the case of strongly bonded systems,[44,45] may not be reliable even at the GGA level. There is still a tendency to overbind such situations with currently available functionals. Hence, we are not overly concerned that the experimental results[23] showed no reactivity of Cr with N_2. A quantitative treatment must await the development of improved functionals. Calculations with highly accurate methods such as CCSD(T) are desirable.

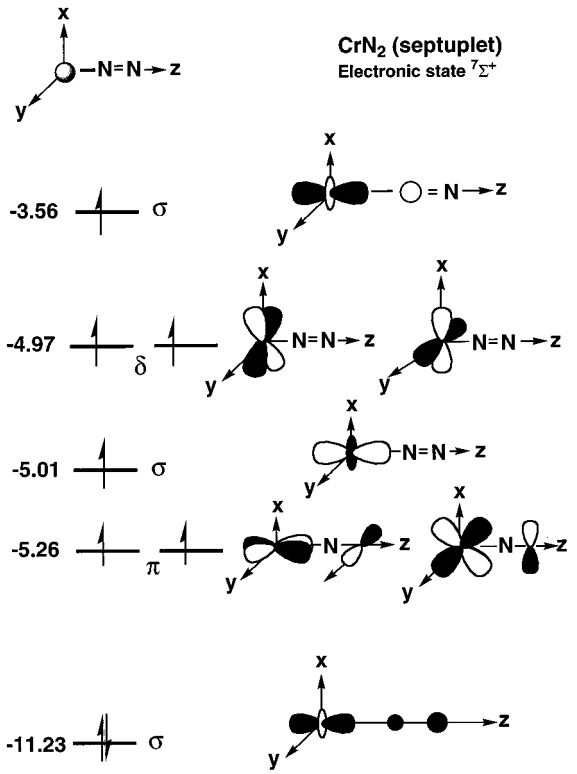

Figure 4. Valence molecular orbital diagram for the ground state of CrN_2. Symmetries, eigenvalues (in eV), and occupation numbers are presented.

In Table 3, it can be seen that the vibrational harmonic frequencies are positive, indicating that the structures are minima on the different PESs. The calculated frequencies could help guide future experimental characterization of some of these states, provided they can be isolated. Note that the N−N bond distances as well as the highest frequencies of these structures indicate that the N−N bond is weakened from the first to the third structure in Table 3.

In Figure 4, the molecular orbital diagram of the ground state of CrN_2 is presented. The electronic state for this system is $^7\Sigma^+$, and the singly occupied orbitals are mainly on the Cr atom.

The behavior of the Cr atom with the N_2 molecule is similar to that shown by the Mo atom interacting with N_2.[28] In both systems, the N_2 molecule is very weakly bonded to the transition metal atom, and as was the case with H_2, a definite conclusion about the reactivity of Cr and N_2 is not yet possible.

The results presented above are in good agreement with the experimental observation by Parnis et al.[23] that reported a generally low reactivity of Cr atoms with respect to closed-shell molecules.

C. Geometry Optimization of CrO_2. As with H_2 and N_2, several initial geometries and multiplicities were used, and several critical points on the different PESs were found. The optimized geometries of CrO_2 are shown in Figure 5. Bond distances at the LSD level and energy differences at the GGA level with respect to the dissociation limit ($Cr(^7S) + O_2$) are also shown.

In contrast with CrH_2 and CrN_2, for CrO_2 Figure 5 indicates that there are several local minima that are thermodynamically stable. For the nonet state no minima were found, so this PES will be excluded from the following discussion. The ground state is a triplet bent structure that has a binding energy of 125.6 kcal/mol. The most stable structures, triplet and quintet, of CrO_2 have lost the covalent O−O bond, in favor of Cr−O bonding.

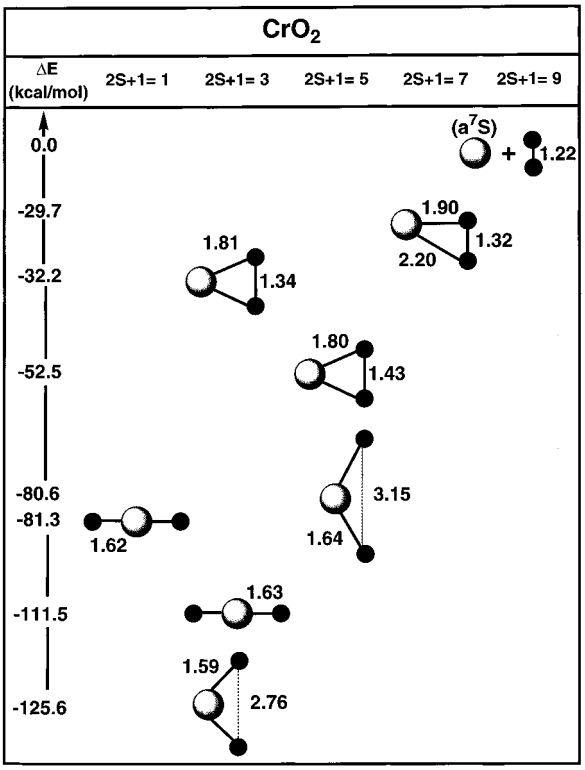

Figure 5. Optimized geometries of CrO_2 for different spin multiplicities. The geometries were obtained at the LSD level (Vosko, Wilk, and Nusair[32]), by minimization of the total energy, without symmetry constraints. Bond distances (in Å) and energy differences (in kcal/mol) at the GGA level (Perdew and Wang for exchange[33] and Perdew for correlation[34,35]) are also shown. The GGA results are single-point calculations with the geometry optimized at the LSD level.

The bent structure is the most stable structure on the triplet, quintet, and septet PES. For the singlet state, the bent minimum (not in Figure 5) is located at 15.9 kcal/mol below the dissociation limit. This structure presents the O_2 molecule molecularly bonded to the Cr atom. On the singlet PES, the linear structure is more stable than the bent structure. For all PESs with different spin multiplicities that were studied, except the singlet one, the general behavior is that the linear structures (not in Figure 5) are less stable than the bent structures.

The ground state of CrO_2 is a triplet followed by a quintet. Comparing the triplet and the quintet bent sructures, it can be seen that the Cr−O bond distance is similar, but the O−O bond length increases with the multiplicity. In this case, it seems that the molecular orbitals of the O_2 molecule are affected by the exchange of spin multiplicities. The covalent bonds between the Cr atom and the oxygen atoms are formed while the spins pair up, reducing the overall multiplicity. The effect of chemisorption on the metal magnetism has also been studied by Fournier et al.[41]

In Figure 5 the septet bent structure is completely distorted. The O−O bond distance is longer than the O−O bond distance of the isolated molecule, but it is not dissociated. The distortion of this structure will be explained with the molecular orbitals analysis at the end of this section.

On the triplet and quintet PES, there are other bent minima with the O_2 molecularly bound to the Cr atom. These structures are more stable than the dissociation limit by 32.2 and 52.5 kcal/mol, for the triplet and the quintet PES, respectively. The GGA energy difference between the two bent triplet structures (molecular and dissociative) is 93.4 kcal/mol. The GGA energy difference between the two bent quintet structures (molecular

TABLE 4: Molecular Structures, Spin Multiplicities, and Relative Energies (in kcal/mol) at the LSD Level (Vosko, Wilk, and Nusair[32]) and at the GGA Level (Perdew and Wang for Exchange[33] and Perdew for Correlation[34,35]), Harmonic Frequencies (in cm^{-1}), and the Assignment by Symmetry of the Most Stable Geometries of Nonet, Septet, Quintet, and Triplet Spin States of CrO_2[a]

Structure	2S+1	ΔE(LSD) (Kcal/mol)	ΔE(GGA) (Kcal/mol)	ν (cm^{-1})	A
+ 1.22	9	0.0	0.0		
1.90, 1.32, 2.20	7	-34.9	-29.7	270 564 1198	a' a' a'
3.15, 1.64	5	-83.8	-80.6	132 732 838	a_1 b_1 a_1
2.76, 1.59	3	-137.6	-125.4	277 1018 1056	a_1 a_1 b_1

[a] The GGA results are single-point calculations with the geometry optimized at the LSD level. Vibrational studies were performed at the LSD level (Vosko, Wilk, and Nusair[32]).

and dissociative) is 28.1 kcal/mol. These results indicate that the dissociative reaction of O_2 with the Cr atom is strongly preferred over the molecular adsorption.

In Table 4 the information for CrO_2 is summarized. The stability order is the same at the LSD and GGA levels. The C_{2v} structures are the most stable ones for the triplet and the quintet PES. For the septet spin state, the most stable structure has C_s symmetry. All the structures are thermodynamically stable. The energy differences with respect to the dissociation limit ($Cr(^7S) + O_2$) are very large for all the C_{2v} structures that are reported in Figure 5 and Table 4. For the distorted septet, the energy difference is not as large as for the other triangular structures.

Also in Table 4, the vibrational analysis obtained at the LSD level for the most stable CrO_2 structures is presented. For the septet bent structure, the first two normal modes of vibration indicate that the two Cr−O bond distances are different. For the quintet most stable structure, the O−O bond length is longer than the O−O bond distance for the triplet ground state, and the vibrational analysis reflects this difference. This information could be useful for future experimental work on this system.

The comparison between these results and the previous results of the Mo atom[28] shows that the general behavior is quite similar, the ground state being the triplet bent structure for both systems. The most important difference is on the singlet PES, where the ground state is a bent structure for MoO_2 and a linear structure for CrO_2.

According to the present results, in the reaction of the Cr atom with O_2, the first step is a weak adsorption of the O_2 (triplet) on the Cr atom on the septet surface. This step occurs when an α electron is formally transferred from the Cr atom into the antibonding π^* system of the O_2 molecule. The electron transfer is connected with a spin flip, which changes the multipicity from a nonet to a septet. This charge-transfer step stabilizes the system considerably and breaks the C_{2v} symmetry.

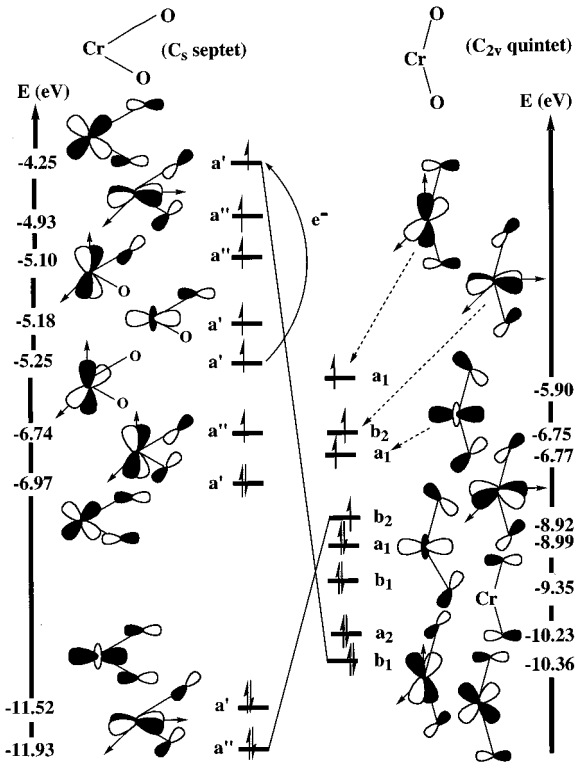

Figure 6. Correlation molecular orbitals diagram of the CrO_2 (septet and quintet) with C_s and C_{2v} symmetry, respectively. Symmetries and eigenvalues (in eV) at the GGA level (Perdew and Wang for exchange[33] and Perdew for correlation[34,35]) are presented. The GGA results are single-point calculations with the geometry optimized at the LSD level. The spin flip is indicated by an arrow in the orbital diagram of the septet.

In Figures 6 and 7, the molecular orbital diagrams of the most stable CrO_2 structures on the septet, quintet, and triplet PES of CrO_2 are presented. In the molecular orbital diagram of the CrO_2 septet (left side of Figure 6), the lowest lying molecular orbitals are bonding between the Cr atom and the molecule and bonding within the molecule. The next class of molecular orbitals are bonding between the Cr and the molecule and antibonding within the molecule. The majority of the other orbitals are nonbonding. The highest occupied orbitals are antibonding between the Cr atom and the molecule and antibonding within the molecule. The comparison between the septet and the quintet minimum of CrO_2 (right side of Figure 6) could be possible if we consider that the classification of the orbitals changes due to the change in the geometry. As an example, the highest occupied orbital of the CrO_2 septet is antibonding between the Cr atom and O_2 and antibonding in the O_2. From the orbital topography we can assign this orbital to the lowest orbital of the CrO_2 quintet that is reported in Figure 6. The explanation for this shift of the orbitals is the fact that the antibonding δ-type orbital from the side-on complex of the CrO_2 septet changes to a bonding π-type orbital in the CrO_2 quintet. This change of side-on complex orbitals to Cr−O bonding orbitals is the reason for the energetic stabilization of the CrO_2 quintet compared with the septet.

In Figure 7 the molecular orbital correlation diagram from the CrO_2 quintet to the triplet ground state is presented. The topography of the orbitals changes slightly from the quintet to the triplet. However, some π-bonding orbitals between the oxygens in the quintet are substituted by σ bonding in the triplet. This change of bonding results in a shorter distance between the two oxygen atoms in the triplet compared to the quintet.

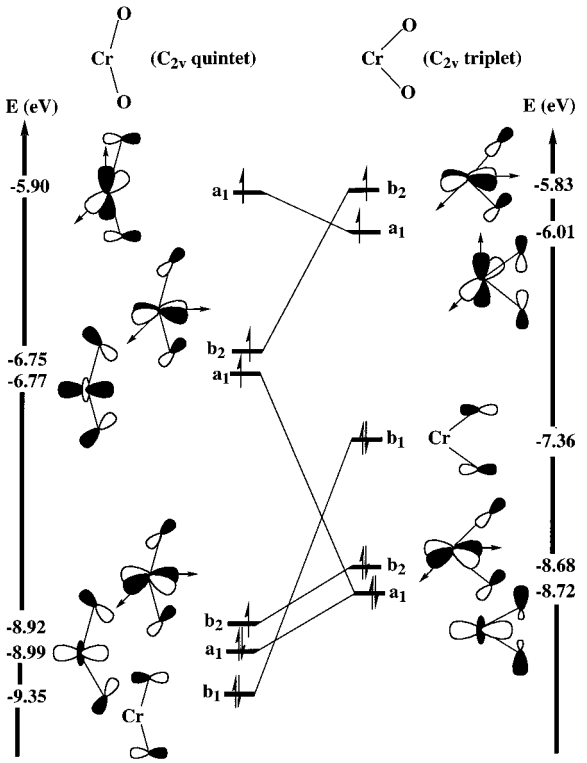

Figure 7. Correlation molecular orbitals diagram of the CrO_2 (quintet and triplet) with C_{2v} symmetry. Symmetries and eigenvalues (in eV) at the GGA level (Perdew and Wang for exchange[33] and Perdew for correlation[34,35]) are presented. The GGA results are single-point calculations with the geometry optimized at the LSD level.

For the MoO_2 system the same reaction mechanism was found,[28] the molecular orbital pictures for systems CrO_2 and MoO_2 being quite similar.

The experimental results of Parnis and co-workers[23] lead to several conclusions concerning the nature of the interactions between Cr and O_2. The limiting high-pressure, second-order rate constant is close to the gas-kinetic collision frequency, which indicates that no significant energy barriers exist to the formation of the CrO_2 product. This system is known from high-temperature mass spectrometric studies[46,47] that have provided information on the dissociation energy relative to Cr + O_2 (113 ± 11 kcal/mol). From the description in the JANAF tables, CrO_2 is a strongly bound dioxide species, with an estimated O−Cr−O bond angle of 110° and with the ground electronic state equal to $^3A_1$ in C_{2v} symmetry. Parnis et al.[23] used this information to calculate the rate constant. They used different models and set of vibrational frequencies leading to different conclusions, and hence, they concluded that further characterization of the Cr + O_2 reaction product is needed before a decision can be made as to which of the models is preferred. The large value of the low-pressure recombination rate constant for Cr + O_2 from the Parnis et al.[23] study indicates that the reaction product is strongly bound, with a binding energy greater than 60 kcal/mol.

On the other hand, reactions of laser-ablated Cr atoms with O_2 plus density functional calculations of geometry and vibrational frequencies for CrO_2 isomers using the B3LYP approximation at low cost were recently reported by Chertihin et al.[48] The experimental and theoretical angle that they reported is 128° ± 4 and 125°, respectively. The theoretical ground electronic state is $^3B_1$ in C_{2v} symmetry. They also reported a good agreement between calculated and observed spectra.

TABLE 5: Results of CrO_2 (Triplet): Theoretical (LSD approximation of This Work and B3LYP Approximation of Chertihin et al.[48]) and the Experimental Data Used for the Calculations of the Rate Constant by Parnis et al.[23]

LSD approximation	B3LYP approximation	experimental data
C_{2v}	C_{2v}	C_{2v}
$^3B_2$	$^3B_1$	$^3A_1$
Cr−O = 1.59 Å	Cr−O = 1.586 Å	Cr−O = 1.627 Å
O−Cr−O = 120.5°	O−Cr−O = 125°	O−Cr−O = 110°
E_0 = 125.6 kcal/mol		E_0 = 113 ± 11 kcal/mol
1056 cm^{-1}	1071 cm^{-1}	1008 cm^{-1}
277 cm^{-1}	276 cm^{-1}	300 cm^{-1}
1018 cm^{-1}	1025 cm^{-1}	998 cm^{-1}

The theoretical and experimental data used for the calculations of the rate constant by Parnis et al.[23] of CrO_2 are summarized in Table 5. As can be seen, symmetry, geometries, binding energies, and vibrational modes are in good agreement. The most important difference is in the electronic states, which are $^3B_2$ from the results of this work, $^3B_1$ from DFT calculations using the B3LYP approximation,[48] and $^3A_1$ from the experimental values. The difference in the theoretical electronic configuration is due to the different orientation of the molecule. The results of both theoretical approximations are in good agreement.

The theoretical characterization of the Cr + O_2 reaction product indicates that the reaction product is strongly bound, in agreement with the experimental results. Since the uncertainties on vibrational frequencies and electronic structure could lead to some problems with the calculations of the rate constants,[23] the calculated frequencies and electronic states in Table 5 could be a hepful guide for future experimental characterization of this system.

Throughout this work, note that the resulting minima are strongly sensitive to the choice of starting test geometries. For this reason we cannot exclude the possibility that the global minima were missed in the optimization procedure. Nevertheless the number of initial geometries (with different bond distances, angles, and symmetry) that were considered is sufficiently high to feel confident that they are not far away from the true absolute minimum.

Summary and Conclusions

A density functional study of the reaction between a Cr atom and H_2, N_2, and O_2 is presented. For the geometry optimization, the local spin density approximation (LSD) can be used. As it is already well-known, GGA potentials must be used to obtain the correct energetic order of the optimized structures.

The reactions of a Cr atom with H_2, N_2, and O_2 were studied in order to obtain an explanation of the different observed reactivities. For this study, we scanned the different PESs of these reactions to find local minima. For CrH_2 and CrN_2, only one local minimum under the dissociation limit was found. For CrH_2, the ground state is a quintet bent structure and the electronic state is $^5B_1$. For CrN_2, the ground state is a septet linear structure and the electronic state is $^7\Sigma^+$. Both structures are very weakly bonded, and hence, no definite conclusion regarding the Cr−H_2 and Cr−N_2 reactivities can be stated.

For CrO_2, several local minima that are thermodynamically stable were found on the septet, quintet, triplet, and singlet PES. The lowest minimum is a bent structure on the triplet PES. The electronic state for this system is $^3B_2$. For this system, a two-step reaction path, which goes over the bent minimum on the septet PES to the bent minimum on the quintet one, is suggested. This structure can be stabilized in a following step, changing

from the quintet to the triplet bent structure. The breaking of the C_{2v} symmetry in the septet minimum is very interesting. The analysis of the molecular orbitals shows that this symmetry breaking is due to the partial filling of the antibonding π^* orbital in the O_2 molecule. For this system, the covalent bonds are formed while the spins pair up, reducing the overall multiplicity.

It is also concluded that the different reactivities of H_2, N_2, and O_2 with the Cr atom are due to the different bond strengths of these molecules. For the CrO_2 system, the O_2 molecule is completely dissociated after two spin flips, and the Cr−O bonds are formed. For CrH_2 and CrN_2, the molecules are weakly bonded to the Cr atom. The Cr atom is always the electron donor in these reactions.

The behavior of the Cr atom with the H_2, N_2, and O_2 is quite similar to that shown by the Mo atom interacting with this molecules.

The theoretical explanation of some of the available experimental results provide a better understanding of the electronic structure and the reaction mechanism of the Cr atom with H_2, N_2, and O_2.

Acknowledgment. The author would like to thanks Dennis R. Salahub and Andreas M. Köster for helpful discussions. I would like to acknowledge the Laboratorio de Supercomputo y Visualizacion en Paralelo at UAM-Iztapalapa (México) for providing computer time on the Silicon Graphics Power Challenge Computer, and DGSCA/UNAM (México) for providing computer time on the CRAY YMP 4/432.

References and Notes

(1) Bauschlicher, C. W.; Langhoff, S. R. *Int. Rev. Phys. Chem.* **1990**, *9*, 149.
(2) Veillard, A. *Chem. Rev. (Washington, D.C.)* **1991**, *91*, 743.
(3) Hintermann, A.; Manninen, M. *Phys. Rev. B* **1983**, *27*, 7262.
(4) Ekardt, W. *Phys. Rev. B* **1988**, *37*, 9993.
(5) Upton, T. H. *Phys. Rev. Lett.* **1986**, *56*, 2168.
(6) Robles, J.; Iniguez, M. P.; Alonso, J. A.; Mananes, A. *Z. Phys. D* **1989**, *13*, 269.
(7) Fournier, R. In *The 5th International Conference on the Applications of Density Functional Theory in Chemistry and Physics*; *Int. J. Quantum Chem.* **1994**.
(8) Siegbahn, P. E. M.; Blomberg, M. R. A.; Bauschlicher, C. W. *J. Chem. Phys.* **1984**, *81*, 1373.
(9) Ruiz, M. E.; Garcia-Prieto, J.; Novaro, O. *J. Chem. Phys.* **1984**, *80*, 1529.
(10) Garcia-Prieto, J.; Ruiz, M. E.; Poulain, E.; Ozin, G. A.; Novaro, O. *J. Chem. Phys.* **1984**, *81*, 5920.
(11) Garcia-Prieto, J.; Ruiz, M. E.; Novaro, O. *J. Am. Chem. Soc.* **1985**, *107*, 5635.
(12) Novaro, O.; Garcia-Prieto, J.; Poulain, E.; Ruiz, M. E. *J. Mol. Struc. (Theochem)* **1986**, *135*, 79.
(13) Balasubramanian, K. *Chem. Phys. Lett.* **1987**, *135*, 288.
(14) Balasubramanian, K.; Feng, P. Y.; Liao, M. Z. *J. Chem. Phys.* **1988**, *88*, 6955.
(15) Balasubramanian, K.; Wang, J. Z. *J. Chem. Phys.* **1989**, *91*, 7761.
(16) Li, J.; Balasubramanian, K. *J. Phys. Chem.* **1990**, *94*, 545.
(17) Poulain, E.; Colmenares-Landin, F.; Castillo, S.; Novaro, O. *J. Mol. Struct. (THEOCHEM)* **1990**, *210*, 337.
(18) Martinez-Magadan, J. M.; Ramirez-Solis, A.; Novaro, O. *Chem. Phys. Lett.* **1991**, *186*, 107.
(19) Colmenares-Landin, F.; Castillo, S.; Martinez-Magadan, J. M.; Novaro, O.; Poulain, E. *Chem. Phys. Lett.* **1992**, *189*, 378.
(20) Sanchez, M.; Ruette, F.; Hernandez, A. J. *J. Phys. Chem.* **1992**, *96*, 823−828.
(21) Siegbahn, P. E. M.; Blomberg, M. R. A. *Chem. Phys.* **1984**, *87*, 189.
(22) Bauschlicher, C. W.; Pettersson, L. G. M.; Siegbahn, P. E. M. *J. Chem. Phys.* **1987**, *87*, 2129.
(23) Parnis, J. M.; Mitchell, S. A.; Hackett, P. A. *J. Phys. Chem.* **1990**, *94*, 8152 and references therein.
(24) Parnis, J. M.; Mitchell, S. A.; Rayner,. M.; Hackett, P. A. *J. Phys. Chem.* **1988**, *92*, 3869.
(25) Parnis, J. M.; Mitchell, S. A.; Hackett, P. A. *Chem. Phys. Lett.* **1988**, *151*, 485.
(26) Mitchell, S. A.; Simard, B.; Rayner, D. M.; Hackett, P. A. *J. Phys. Chem.* **1988**, *92*, 1655.
(27) Mitchell, S. A.; Hackett, P. A.; Rayner, D. M.; Cantin, M. *J. Phys. Chem.* **1986**, *90*, 6148.
(28) Martínez, A.; Köster, A. M.; Salahub, D. R. *J. Phys. Chem.* **1997**, *101*, 1532.
(29) Lian, L.; Mitchell, S. A.; Rayner, D. M. *J. Phys. Chem.* **1994**, *98*, 11637.
(30) *DEMON. User's guide*, version 1.0 beta, Biosym Technologies: San Diego, 1992.
(31) Köster, A. M.; Leboeuf, M.; Salahub, D. R. *deMon* Properties; Universitéde Montreal, 1995.
(32) Vosko, S. H.; Wilk, L.; Nusair, M. *Can. J. Phys.* **1980**, *58*, 1200.
(33) Perdew, J. P.; Wang, Y. *Phys. Rev. B* **1986**, *33*, 8800.
(34) Perdew, J. P. *Phys. Rev. B* **1986**, *33*, 8822.
(35) Perdew, J. P. *Phys. Rev. B* **1986**, *34*, 7406E.
(36) Godbout, N.; Salahub, D. R.; Andzelm, J.; Wimmer, E. *Can. J. Chem.* **1992**, *70*, 560.
(37) Becke, A. D. *J. Chem. Phys.* **1988**, *88*, 2547.
(38) Schlegel, H. B. *Ab initio Methods in Quantum Chemistry-I*; Wiley: New York, 1987.
(39) Martínez, A.; Vela, A.; Salahub, D. R. *Int. J. Quantum Chem.* **1997**, *63*, 301.
(40) Morse, C. E. *Atomic Energy Levels. As Derived from the Analyses of Optical Spectra*; United States Department of Commerce, National Bureau of Standards: Washington, DC, 1949.
(41) Fournier, R.; Andzelm, J.; Goursot, A.; Russo, N.; Salahub, D. R. *J. Chem. Phys.* **1995**, *93*, 2919.
(42) Xiao, Z. L.; Hauge, R. H.; Margrave, J. L. *J. Phys. Chem.* **1992**, *96*, 636−644.
(43) Ruiz, E.; Salahub, D. R.; Vela, A. *J. Am. Chem. Soc.* **1995**, *117*, 1141.
(44) Salahub, D. R.; Fournier, R.; Mlynarski, P.; Papai, I.; St-Amant, A.; Ushio, J. In *Density Functional Methods in Chemistry*; Labanowski, J., Andzelm, J., Eds.; Springer-Verlag: Berlin, 1991.
(45) Ziegler, T. *Chem. Rev. (Washington, D.C.)* **1991**, *91*, 651.
(46) *JANAF Thermochemical Tables, 3rd ed.*; Dow Chemical Co.: Midland, MI, 1985.
(47) *J. Phys. Chem. Ref. Data* **1985**, *14* (Suppl. 1).
(48) Chertihin, G. V.; Bare, W. D.; Andrews. L. *J. Chem. Phys.* **1997**, *107*, 2798.